

Temperature dependence of the spectra of optical constants of CdTe in the region of the absorption edge

© V.A. Shvets^{1,2}, D.V. Marin^{1,2}, M.V. Yakushev¹, S.V. Rykhliitskii¹

¹Rzhanov Institute of Semiconductor Physics, Siberian Branch, Russian Academy of Sciences, 630090 Novosibirsk, Russia

²Novosibirsk State University, 630090 Novosibirsk, Russia

e-mail: shvets@isp.nsc.ru

Received July 16, 2023

Revised September 14, 2023

Accepted October 01, 2023

In this work, the spectra of optical constants of epitaxial layers of cadmium telluride near the fundamental absorption edge are studied. For this purpose, ellipsometric measurements of the layers under study were carried out in a vacuum chamber in the temperature range from $T = 38^\circ\text{C}$ to 275°C . A numerical algorithm has been developed for solving the inverse ellipsometry problem for the structures under consideration, with the help of which the spectral dependences of the refractive index $n(\lambda)$ and absorption index $k(\lambda)$ are determined in the wavelength range from 700 to 1000 nm. The parametric dependences of $k(\lambda, T)$ in the fundamental absorption region and in the transparency region are presented. The presence of an extended absorption tail in the transparency region was established, presumably associated with imperfections in the crystal structure.

Keywords: ellipsometry, cadmium tellurium, spectra of optical constants, fundamental absorption edge, temperature.

DOI: 10.61011/EOS.2023.09.57342.4866-23

1. Introduction

Cadmium telluride is a semiconductor with band gap $E_0 \approx 1.5$ eV. It finds application in solar power engineering, the design of X-ray radiation detectors, and several other branches of industry. Specifically, CdTe layers are used as a buffer in molecular-beam epitaxy (MBE) of mercury cadmium telluride solid solutions for matching of lattice constants. The optical properties of crystalline CdTe have been examined at room temperature [1] and within a wide temperature range [2]. The authors of these papers have presented experimental data and performed a detailed theoretical analysis of the specific features of dielectric function $\varepsilon(E)$ of crystalline CdTe. Various ways to define $\varepsilon(E)$ analytically have been examined: the oscillator model, the dielectric function model (MDF), and the standard critical points model. This *ab initio* theoretical description reproduces the overall shape of function $\varepsilon(E)$ within a wide spectral range, but does not provide a close fit to experimental data.

At the same time, exact values of refraction $n(\lambda)$ and absorption $k(\lambda)$ indices in the chosen spectral region (specifically, near the fundamental absorption edge) are required in a number of applied problems. These data are crucial for material characterization, since optical properties are sensitive to crystalline perfection, the presence of impurity inclusions, mechanical stresses, temperature, and other physical factors.

The specific features of spectra in the region of the absorption edge for CdTe films synthesized in various

ways have been examined in [3–5]. An ellipsometric method of *in situ* temperature measurements for MBE process monitoring has been developed in [6,7] based on the temperature dependence of the fundamental absorption band edge. Absorption band edge λ_0 was distinguished by the onset of interference oscillations of ellipsometric parameters Ψ and Δ on the grown CdTe layer. With this edge identification technique, the accuracy of the developed methods was on the order of 0.5 nm. This accuracy may be enhanced by determining λ_0 from the reconstructed absorption index $k(\lambda)$ profile instead of Ψ , Δ oscillations. The shape of the $k(\lambda)$ dependence near the fundamental absorption edge and in the Urbach tail region also provides valuable insights into the crystalline perfection of the examined material [8]. In addition, a database of $n(\lambda)$ and $k(\lambda)$ is relevant to numerical modeling for photometric and ellipsometric applications.

All these considerations motivate in-depth research into the optical constants of CdTe in the indicated spectral region. In the present study, the results of ellipsometric measurements for thin cadmium telluride layers grown by MBE are reported, and a mathematical algorithm for determining the spectra of optical constants $n(\lambda)$ and $k(\lambda)$ and their temperature dependence near the absorption edge is detailed.

2. Experimental

An MBE setup discussed in detail in [9] was used to grow CdTe films on a Si substrate with a 40-nm-thick

ZnTe buffer layer. The growth process was monitored with a built-in spectral ellipsometer. The thickness of CdTe films was estimated at $\sim 6\ \mu\text{m}$ based on the growth rate, which was determined from ellipsometric data, and the growth time. Ellipsometric measurements were performed for grown samples without contact with the atmosphere (in a vacuum chamber under a residual pressure on the order of 10^{-6} Torr). The samples were heated by thermal radiation from a furnace positioned in the immediate vicinity. Their temperature was determined based on ellipsometric spectra in accordance with the procedure outlined in [6,7].

The ellipsometer was operated in the static mode [10] within the 350–1100 nm range. The 700–1000 nm spectral range, which contains the CdTe absorption edge, was examined in the present study. Measurements were performed with a spectrum scan step of 1 nm. The spectral resolution was ~ 5 nm. The time of measurement of a complete ellipsometric spectrum was 36 s. The accuracy of determination of ellipsometric parameters was $\delta\Psi = 0.05^\circ$ and $\delta\Delta = 0.1^\circ$, and the long-term stability was 0.01° .

3. Specific features of solving the inverse ellipsometry problem

Figure 1 presents the spectra of ellipsometric parameters for the Si/ZnTe/CdTe sample with CdTe layer thickness $d \approx 6\ \mu\text{m}$. These spectra are related to optical constants and layer thicknesses by the well-known ellipsometry equation [11] that may be presented in a symbolic form:

$$\text{tg } \Psi(\lambda) e^{i\Delta(\lambda)} = F(n(\lambda), k(\lambda), d). \quad (1)$$

The optical model characterized by Eq. (1) included a ZnTe layer with a thickness of 40 nm, a CdTe layer, and a surface layer that reproduced the roughness of CdTe. The dashed curve in Fig. 1 is the calculated $\Delta(\lambda)$ spectrum in the absorption region. The optical constants of CdTe and ZnTe needed for calculations were taken from [12]. The observed discrepancy between measured and calculated spectra is rectified by introducing a surface layer with thickness $d_{ox} = 1.3$ nm, which is needed to factor in the roughness parameters, into the model. The optical constants of this layer were determined in accordance with the Bruggeman model [13].

If the thickness of ZnTe and CdTe layers and the surface layer is known, the problem of determination of n and k from Eq. (1) at a given wavelength is a well-posed one and may be solved numerically. We used a proprietary iterative algorithm based on the calculation of the target vector in the domain of required parameters. However, a problem of uniqueness of solution arises when this algorithm is executed. Dots in Fig. 2 denote the values of refraction index n within the interval from 2.95 to 3.15 that are the solutions of Eq. (1) for the experimental spectra from Fig. 1. These solutions were found by a straightforward exhaustive search through the values of n within the indicated interval

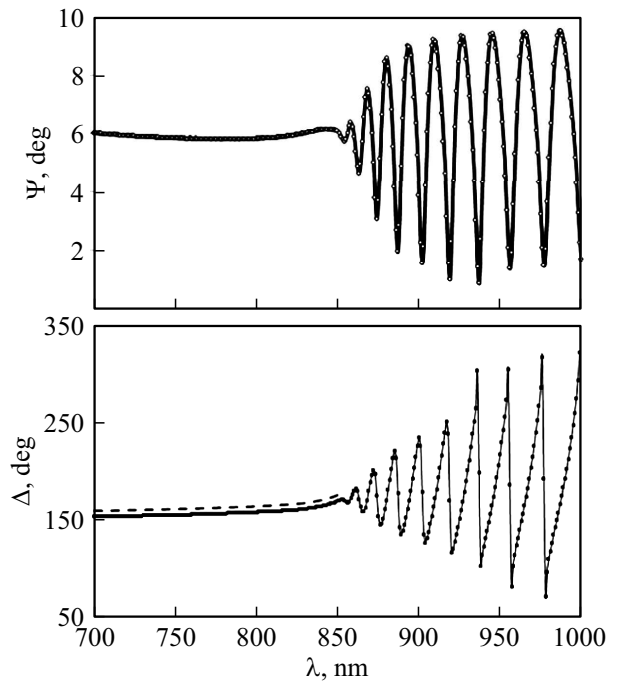


Figure 1. Spectra of ellipsometric parameters measured for the CdTe $6\ \mu\text{m}$ layer.

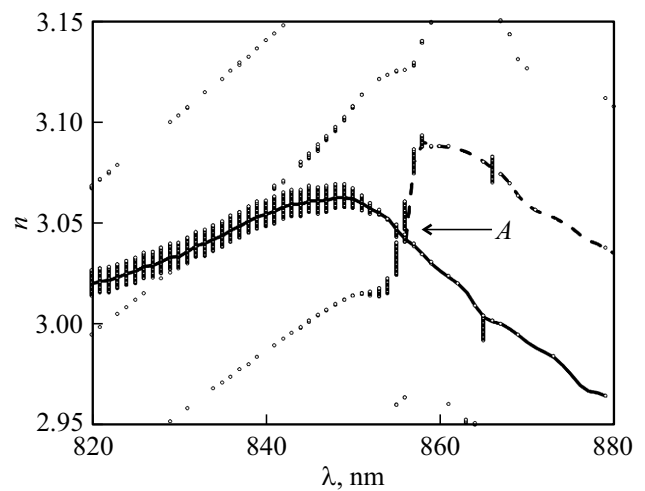


Figure 2. Possible solutions n for the sample with its $\Psi(\lambda)$ and $\Delta(\lambda)$ spectra shown in Fig. 1 (symbols). The solid curve is one of the search algorithm execution branches. The dashed curve represents a probable transition to a neighboring branch, which crosses the chosen branch at point A.

(with step size $\delta n = 5 \cdot 10^{-4}$) and a search through k within the interval from 0 to 0.2 with the same step.

A pair of (n, k) values was considered to be a proper solution if target function $S = (\Psi_{\text{meas}} - \Psi_{\text{calc}})^2 + 0.5(\Delta_{\text{meas}} - \Delta_{\text{calc}})^2 < 0.005$, where Ψ_{meas} , Ψ_{calc} , Δ_{meas} , and Δ_{calc} are the measured and calculated values of ellipsometric parameters expressed in degrees, was obtained by inserting this pair into Eq. (1). It can be seen from Fig. 2 that several solutions may exist

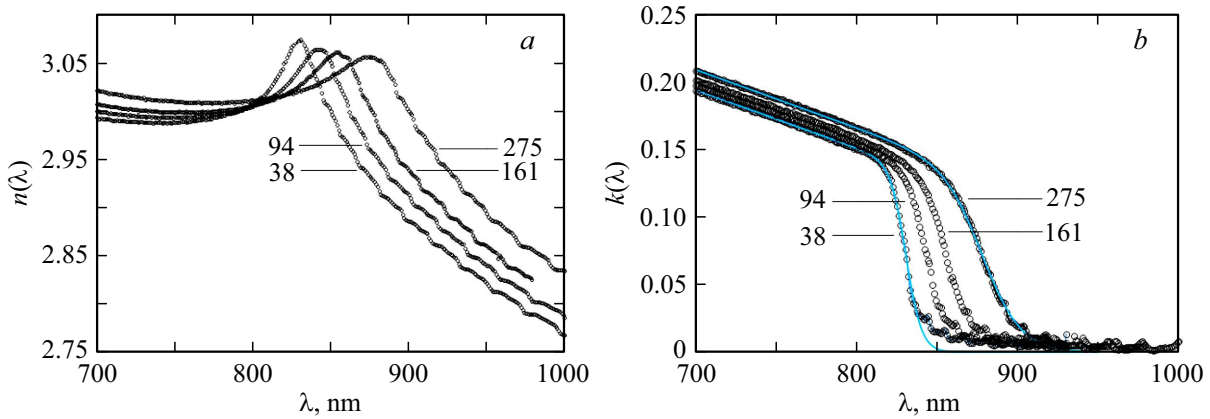


Figure 3. Spectral dependences of refraction (a) and absorption (b) indices calculated based on experimental data for various temperatures that are indicated (in degrees Celsius) next to the corresponding symbol curves. Solid curves represent the approximation of experimental $k(\lambda)$ spectra by formula (3).

within a narrow n interval at the chosen wavelength. The evident multiplicity of solution branches is a manifestation of a multitude of interference periods attributable to a considerable thickness of the CdTe layer. The solid curve represents one possible solution provided by the numerical algorithm advancing steadily from shorter wavelengths to longer ones. A problem of numerical searching arises at the point of intersection between two branches (point A in Fig. 2). Having reached this point, the algorithm may switch to a neighboring branch (see the dashed curve in the figure). A break and a derivative jump then emerge in the obtained $n(\lambda)$ dependence. In order to avoid such transitions to neighboring branches, we applied the criterion of smoothness of functions $n(\lambda)$ and $k(\lambda)$ in execution of the algorithm.

4. Temperature dependences of the spectra of optical constants and their parameterization

Using the calculation method discussed above and experimental data, we calculated spectral dependences $n(\lambda)$ and $k(\lambda)$ within the temperature range from 38 to 275°C. Certain example curves are presented in Fig. 3. As the temperature increases, the spectra of n and k shift toward longer wavelengths and broaden around λ_0 . It is noteworthy that weak oscillations manifest themselves in the transparency region at $\lambda > \lambda_0$ in the calculated spectra. These oscillations are attributable to the ellipsometric measurement uncertainty arising due to restrictions associated with the coherence length of a spectral line. The spectral band of the ellipsometer (5 nm) does indeed cover a considerable part of an interference period, which, according to the data from Fig. 1, is on the order of 20 nm. This affects the accuracy of measurement of ellipsometric spectra and leads to distortion of calculated $n(\lambda)$ and $k(\lambda)$ functions. In subsequent

interpretation of the measurement data, smoothing and averaging of oscillations was performed.

The absorption index spectrum is of principal interest in the context of characterization of the material properties. A $k(\lambda, T)$ dependence in a parametric form is useful in various applied problems. According to the Kane model, absorption coefficient $\alpha = 4\pi k/\lambda$ for direct-gap semiconductors in the region of photon energies $E = hc/\lambda$ exceeding band gap energy E_0 is given by [14]

$$\alpha(E) \sim \frac{\sqrt{E - E_0}}{E}.$$

The wavelength dependence of the absorption index then takes the form

$$k \sim \lambda^2 \sqrt{\frac{hc}{\lambda} - E_0}. \tag{2}$$

The obtained experimental $k(\lambda)$ curves are characterized well by this formula only in the immediate vicinity of λ_0 (within ~ 10 nm). Conspicuous is the fact that experimental dependence $k(\lambda)$ remains linear with a fair degree of accuracy within the 700–800 nm range. If one discards band theory calculations and instead tries to find a proper analytical dependence to characterize experimental data, a fine fit is provided by the following empirical formula:

$$k(\lambda) = \frac{b(1 - A|\lambda - \lambda_0|)}{1 + \exp\left(\frac{\lambda - \lambda_0}{\delta\lambda}\right)}, \tag{3}$$

where A , b , and $\delta\lambda$ are adjustable constants. Their physical meaning is simple: $b = 2k(\lambda_0)$, product Ab sets the slope of the linear spectrum part, and $\delta\lambda$ specifies the broadening of the step. Fitting of the model curves was performed for all measured $k(\lambda)$ spectra, and the temperature dependences of A , b , and $\delta\lambda$ were found. Quantity λ_0 , which characterizes the optical band gap, was also treated as an adjustable parameter in the process. As was noted in [15], the value of λ_0 may be determined by establishing the position of the maximum steepness of dependence $k(\lambda)$. We determined

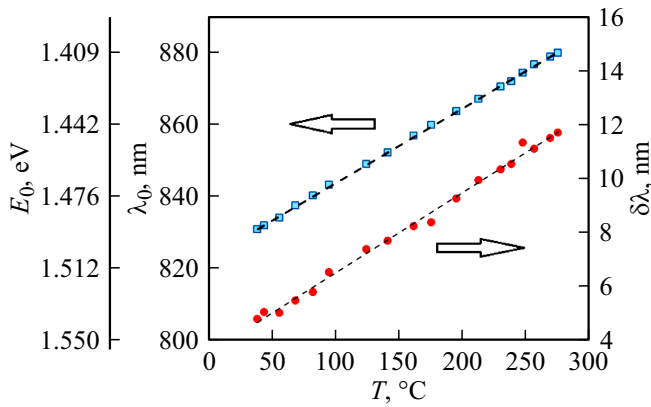


Figure 4. Temperature dependences of absorption edge λ_0 and broadening parameter $\delta\lambda$ (symbols) determined from the approximation of experimental $k(\lambda)$ spectra by formula (3). The dashed line is the linear approximation of experimental dependences. The leftmost vertical scale presents the values of λ_0 in electronvolts.

all four parameters of formula (3) by minimizing difference $F = \sum_{\lambda} (k_{\text{calc}} - k_{\text{exp}})^2$ between calculated and experimental k values in the $\lambda < \lambda_0$ region. The criterion of maximum steepness of experimental $k(\lambda)$ spectra at point $\lambda = \lambda_0$ was satisfied automatically in this case.

The solid curves in Fig. 3 represent the approximations of two experimental $k(\lambda)$ dependences corresponding to the temperatures of 38 and 275°C by formula (3) with the determined optimum values of fitting parameters. This formula provides a very accurate description of behavior of $k(\lambda)$ in the CdTe absorption region at $\lambda < \lambda_0$. The mean-square deviation between the calculated and experimental curves is 10^{-4} , and the maximum deviation does not exceed $2 \cdot 10^{-3}$. The temperature dependences of parameters $\delta\lambda$ and λ_0 are shown in Fig. 4 with approximations by linear functions (temperature is expressed in degrees Celsius)

$$\delta\lambda = 3.55 + 0.0297T, \quad (4)$$

$$\lambda_0 = 823.8 + 0.207T. \quad (5)$$

The leftmost vertical scale presents the values of λ_0 in electronvolts. The linear dependence coefficient for $\lambda_0(T)$ is $3.45 \cdot 10^{-4}$ eV/°C, which is close to the value of $3.57 \cdot 10^{-4}$ eV/°C derived from the experimental data presented in [2].

The temperature dependences for coefficients A and b take the form

$$A = 1.51 \cdot 10^{-3} + 1.28 \cdot 10^{-6}T - 3.3 \cdot 10^{-9}T^2, \quad (6)$$

$$b = 0.137 - 2.44 \cdot 10^{-5}T. \quad (7)$$

Combined with (4)–(7), formula (3) specifies the parametric temperature dependence of the absorption index of CdTe within the wavelength range from 700 nm to λ_0 .

At $\lambda > \lambda_0$, formula (3) provides an adequate fit to experimental $k(\lambda)$ spectra only in the high-temperature

region. The dependence of the absorption coefficient on the photon energy in the transparency region for a direct-gap semiconductor is specified by the Urbach equation [16]:

$$\alpha(h\nu) = \alpha_0 \exp\left(\frac{h\nu - E_0}{W}\right),$$

where $E_0 = \frac{hc}{\lambda_0}$ is the optical band gap and W is the Urbach energy that sets the rate of decay of the exponential function. It follows that the absorption index should satisfy equation

$$k(\lambda) = C\lambda \exp\left(\frac{(\lambda_0 - \lambda)E_0}{\lambda W}\right). \quad (8)$$

Constant C in (8) is determined from the matching condition for formulae (3) and (8) at point $\lambda = \lambda_0$: $C = b/2\lambda_0$. Attempts at characterizing the experimental $k(\lambda)$ curve in the transparency region with this exponential dependence failed. The dashed curves in Fig. 5 are the result of calculations by formula (8) at different Urbach energy values for $T = 38^\circ\text{C}$ and $T = 275^\circ\text{C}$. The exponential dependence is fitting only within the initial section of experimental curves near λ_0 ; the rate of subsequent decay of the absorption coefficient is much slower.

Absorption near the band gap edge is governed by the tail of the density of states and depends on the electron–phonon interaction, crystal structure defects, and the presence of a background impurity and other crystal lattice imperfections. Dynamic (governed by the phonon spectrum) and static (associated with defects and temperature-independent) components are distinguished here [17]. Following this concept, we tried to present experimental dependence $k(\lambda)$ as a sum of two terms that are similar to (8) and have different Urbach energies W_1 and W_2 :

$$k(\lambda) = C_1\lambda \exp\left(\frac{(\lambda_0 - \lambda)E_0}{\lambda W_1}\right) + C_2\lambda \exp\left(\frac{(\lambda_0 - \lambda)E_0}{\lambda W_2}\right). \quad (9)$$

Formula (9) contains three fitting parameters, since it still follows from the matching condition that $C_1 + C_2 = b/2\lambda_0$. The solid curves in Fig. 5 are the result of approximation of experimental data by a sum of two exponential functions (formula (9)) with the optimum values of $W_1 = 9.5$ meV and $W_2 = 120$ meV (for $T = 38^\circ\text{C}$) and $W_1 = 21$ meV and $W_2 = 81$ meV (for $T = 275^\circ\text{C}$). The temperature dependences of W_1 and W_2 are shown in Fig. 6. Energy W_1 increases by a factor of 2.5 within the considered temperature interval. This is quite explicable if one assumes that the first term characterizes the contribution of the electron–phonon interaction. In contrast, the value of W_2 decreases slightly as the temperature grows. It is fair to assume that the second term in (9) corresponds to the contribution of structural imperfections. The presence of an extended absorption tail in the band gap may characterize the degree of crystalline perfection of epitaxial CdTe layers. There is no need to solve the inverse ellipsometry problem and calculate dependence $k(\lambda)$ if only a qualitative estimate is required. As was proposed in [6], the decay of absorption

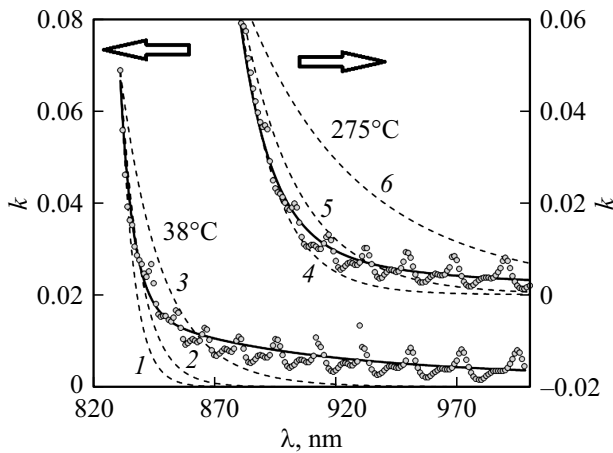


Figure 5. Spectral dependences of absorption index $k(\lambda)$ for $T = 38^\circ\text{C}$ and $T = 275^\circ\text{C}$. Experimental data are represented by symbols, and dashed curves are the result of calculations by formula (8) at different Urbach energy values: $W = 10$ (1), 15 (2), 30 (3), 24 (4), 35 (5) and 70 meV (6). The solid curve is the approximation by a sum of two exponential functions with different Urbach energies.

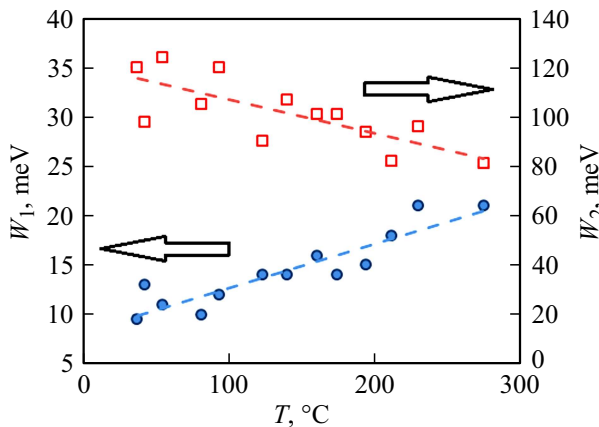


Figure 6. Temperature dependences of energies W_1 and W_2 . Experimental data are represented by symbols, and dashed lines are their linear approximations.

may be evaluated by examining the rate of enhancement of interference oscillations of ellipsometric parameters that occurs as one ventures deeper into the transparency region.

5. Conclusion

Spectra of optical constants of semiconductors contain a wealth of data on their electrophysical characteristics and structural perfection. The method for solving the inverse ellipsometry problem for film structures, which was developed here, provided an opportunity to calculate the spectra of optical constants of epitaxial CdTe layers near the fundamental absorption edge and their temperature dependences.

Analytical formulae presenting the temperature dependence of absorption index spectra in a parametric form were derived. The presence of a weak absorption tail in the transparency region was established. The wavelength dependence of absorption is characterized by a sum of two exponential functions. The first function is associated with the electron–phonon interaction, while the second one specifies the contribution of structural defects. The presence of an extended absorption tail may characterize the degree of crystalline perfection of a material.

Acknowledgments

The authors wish to thank V.A. Volodin for helpful discussions.

Funding

This study was carried out under state assignment of the Ministry of Science and Higher Education of the Russian Federation (project No. 0242-2022-0002).

Conflict of interest

The authors declare that they have no conflict of interest.

References

- [1] S. Adachi, T. Kimura, N. Suzuki. *J. Appl. Phys.*, **74** (5), 3435 (1993). DOI: 10.1063/1.354543
- [2] C.C. Kim, M. Daraselia, J.W. Garland, S. Sivananthan. *Phys. Rev. B*, **56** (8), 4786 (1997). DOI: 10.1103/PhysRevB
- [3] L.A. Kosyachenko, V.M. Sklyarchuk, O.V. Sklyarchuk, O.L. Maslyanchuk. *Semiconductors*, **45** (10), 1273 (2011).
- [4] A.I. Kashuba, B.V. Andrievskcd, H.A. Ilchuk, M. Piasecki, I.V. Semkiv, R.Yu. Petrus. *Zh. Beloruss. Gos. Univ. Fiz.*, **2**, 88 (2021) (in Russian). DOI: 10.33581/2520-2243-2021-2-88-95
- [5] L. Verma, A. Rhare. In: *2022 IOP Conf. Ser.: Mater. Sci. Eng.*, **1263**, 012017. DOI: 10.1088/1757-899X/1120/1/012019
- [6] V.A. Shvets, I.A. Azarov, D.V. Marin, M.V. Yakushev, S.V. Rykhliitsky. *Semiconductors*, **53** (1), 132 (2019). DOI: 10.21883/FTP.2019.01.47001.8947
- [7] D.V. Marin, V.A. Shvets, I.A. Azarov, M.V. Yakushev, S.V. Rykhliitskii. *Infrared Phys. and Technol.*, **116**. Article 103793 (2021). DOI: 10.1016/j.infrared.2021.103793
- [8] Y. Chang, G. Badano, J. Zhao, Y.D. Zhou, R. Ashokan, C.H. Grein, V. Nathan. *J. Electron. Mater.*, **33**, 709 (2004). DOI: 10.1007/s11664-004-0070-5
- [9] Yu.G. Sidorov, S.A. Dvoretiskii, V.S. Varavin, N.N. Mikhailov, M.V. Yakushev, I.V. Sabinina. *Semiconductors*, **35** (9), 1045 (2001).
- [10] E.V. Spesivtsev, S.V. Rykhliitskii, V.A. Shvets. *Optoelectron., Instrum. Data Process.*, **47** (5), 419 (2011).
- [11] R.M.A. Azzam, N.M. Bashara. *Ellipsometry and Polarized Light* (North-Holland, 1977).
- [12] S. Adachi. *Optical constants of crystalline and amorphous semiconductors: Numerical data and graphical information* (Kluwer Academic Publishers, Boston/Dresden/London, 1999). DOI: 10.1007/978-1-4615-5247-5

- [13] D.A.G. Bruggeman. *Ann. Phys.*, **416** (7), 636 (1935).
DOI: 10.1002/andp.19354160705
- [14] H. Kuzmany. *Solid-State Spectroscopy: An Introduction* (Springer-Verlag, Berlin-Heidelberg-N.Y., 1998).
DOI: 10.1007/978-3-642-01479-6
- [15] Y. Chang, S. Guna, C.H. Grein, S. Velicu, M.E. Flatté, V. Nathan, S. Sivananthan. *J. Electron. Mater.*, **36** (8), 1000 (2007). DOI: 10.1007/s11664-007-0162-0
- [16] F. Urbach, *Phys. Rev.*, **92**, 1324 (1953).
- [17] Y. Chang, G. Badano, J. Zhao, Y.D. Zhou, R. Ashokan, C.H. Grein, V. Nathan. *J. Electron. Mater.*, **33**, 709 (2004).
DOI: 10.1007/s11664-004-0070-5

Translated by D.Safin